Reductions, Relative Equilibria, and Bifurcations in the Generalized van der Waals Potential: Relation to the Integrable Cases

Antonio Elipe and Sebastián Ferrer
Grupo de Mecánica Espacial, Departamento de Física Teórica, Universidad de Zaragoza, 50009 Zaragoza, Spain
(Received 2 November 1993)

Complementing the work of Alhassid *et al.* we study the global dynamics of the averaged system of the generalized van der Waals interaction in the reduced space which is a two-dimensional sphere. We find lines of local "pitchfork" and global "oyster" bifurcations emerging from the known integrable cases $\beta = \frac{1}{2}, 1, 2$; this explains the chaos-order-chaos transition. We present the libration and circulation modes of the Runge-Lenz vector and its stability domains. The appearance-disappearance pattern of separatrices for the known integrable cases leads us to conjecture that those are the only ones.

PACS numbers: 31.50.+w, 03.20.+i, 32.60.+i, 34.30.+h

The generalized van der Waals interaction is a dynamical system proposed by Alhassid *et al.* [1] whose Hamiltonian in cylindrical coordinates is

$$\mathcal{H} = \mathcal{H}_0 + \mathcal{P}, \tag{1}$$

with

$$\mathcal{H}_0 = \frac{1}{2}\left(P_\rho^2 + P_z^2 + \frac{P_\phi^2}{\rho^2}\right) - \frac{1}{r}, \qquad \mathcal{P} = \gamma(\rho^2 + \beta^2 z^2),$$

where $r = \sqrt{\rho^2 + z^2}$, P_ρ, P_ϕ, and P_z are the canonical momenta conjugate to the coordinates ρ, ϕ, and z, respectively, with two parameters: γ, which is square of a frequency, and β, which is dimensionless. This Hamiltonian defines a 2 degrees of freedom system because it possesses cylindrical symmetry: ϕ is a cyclic variable and so the momenta P_ϕ is conserved. Since P_ϕ is the z component of the angular momentum, it can be quantized as $P_\phi = m\hbar$, where m is the magnetic quantum number. The system (1) has some special submanifolds as solutions: planar polar solutions $m = 0$, which are functions of β, and include rectilinear solutions along the O-z axis; and equatorial trajectories for which z, Z vanish permanently which define an integrable system of 1 degree of freedom for all values of β.

Hamiltonian (1) represents several cases of physical interest in solid-state physics and physical chemistry. Thus, when $\gamma = 0$, we have the standard hydrogen-atom problem or Coulomb problem. When $\beta = 0$ (and $\gamma = -\omega^2/2$, where ω is the electron cyclotron frequency) we have the quadratic Zeeman effect in moderate or strong magnetic fields and it has been studied extensively (see, for instance, Gay [2] and Hasegawa *et al.* [3]). For $\beta = 1$ we have the integrable spherical quadratic Zeeman effect. If $\beta = \sqrt{2}$ (and $\gamma = -1/16d^3$, where d is the distance from atom to the surface), we have the instantaneous van der Waals potential [4].

The pioneering work of Alhassid *et al.* set up two lines of studies: search for integrals and understanding of the dynamics. For $m = 0$ Ganesan and Lakshmanan [5] found integrals for $\beta = \frac{1}{2}, 2$; numerical and analytical studies of the flow have also been done [5–7]. For $m \neq 0$ Farrelly and Howard [8] have found two integrals $\mathcal{I}_\beta$ for $\beta = \frac{1}{2}, 2$, following the approach of Blümel *et al.* [9] with the Paul trap system. For the sake of completeness we bring the three known integrals, valid for all m, together,

$$\mathcal{I}_1 = \mathcal{I}^2 + \frac{P_\phi^2 z^2}{\rho^2}, \quad \mathcal{I}_2 = -P_\rho \mathcal{I} + \frac{z}{r} - \rho^2 z + \frac{P_\phi^2 z}{\rho^2},$$

$$\mathcal{I}_{1/2}^2 = \left[P_z \mathcal{I} + \frac{\rho}{r} - \frac{\rho z^2}{4} + \frac{P_\phi^2}{\rho}\right]^2 + \frac{P_\phi^2}{\rho^2}\mathcal{J}^2 + P_\phi^2 r^2,$$

where $\mathcal{I} = \rho P_z - z P_\rho$ and $\mathcal{J} = \rho P_\rho + z P_z$. With respect to the global dynamics, some analytical and numerical work has also been done by Ganesan and Lakshmanan [10] and Farrelly and Howard [8] although they mention the need for further investigation. We think this Letter responds precisely to that question, showing the connection with the integrable cases.

We restrict ourselves in what follows to the region of phase space where γ is a small parameter. Alhassid *et al.* explain "the sensitivity of Rydberg atoms to perturbations and the wealth of experimental information they can yield has led to the revival of interest in the study of atoms in external fields." Expressing the Hamiltonian in Delaunay variables [11,12], and after the normalization over the mean anomaly, we get the reduced Hamiltonian [7]. The principal quantum number, that we denote as L, is now an integral. The first order of the new Hamiltonian is precisely the adiabatic invariant found by Alhassid *et al.*,

$$\Lambda = (4 - \beta^2)\|\boldsymbol{A}\|^2 + 5(\beta^2 - 1)A_z^2, \tag{2}$$

where $\boldsymbol{A}$ is the Runge-Lenz vector and A_z is the z component of $\boldsymbol{A}$. This generalizes the one given by Solov'ev [13] and Herrick [14] for the Zeeman effect. In general for each action L the orbital space of the reduced perturbed Coulomb problem is given by $S^2 \times S^2$ (see [15]). Nevertheless for systems that enjoy an axial symmetry Meyer showed [16] (see also [17]) that there is another reduction we can make. In other words, the rotational symmetry maps it onto a conservative system with only 1 degree of freedom. For each pair $(n, m) = (L, H)$ the double re-

0031-9007/94/72(7)/985(4)$06.00

duced orbital space is a two-dimensional sphere S^2, which gives us the dynamics of the Runge-Lenz vector. Earlier work in molecules [18], formally speaking, is closely related; the S^2 representation is applied to rotational and vibrational problems, noticing types of bifurcations similar to the ones found here.

Providing S^2 with a set of global coordinates is another matter. Coffey *et al.* [19] proposed the following global representation:

$$\xi_1 = (\boldsymbol{G} \times \boldsymbol{A})\boldsymbol{k}, \quad \xi_2 = \|\boldsymbol{G}\|\boldsymbol{A}\boldsymbol{k},$$
$$\xi_3 = \frac{\|\boldsymbol{G} \times \boldsymbol{k}\|^2 - \|\boldsymbol{A}\|^2}{2},$$

such that

$$\xi_1^2 + \xi_2^2 + \xi_3^2 = (L^2 - H^2)^2/4, \tag{3}$$

where $\boldsymbol{G}$ is the angular momentum vector. Then, they applied them to explain the bifurcation in the Zeeman effect and the nature of the critical inclination in satellite theory, showing that there are two pitchfork bifurcations of circular orbits. Some authors, choosing local representations of the reduced space on a cylinder, had failed to represent the neighborhoods of circular and equatorial orbits where significant events are expected to occur. We will see more of that in this Letter, where we use these coordinates (ξ_1, ξ_2, ξ_3), referring to them as CDM.

Throughout the interval $0 < \sigma < 1$, where $\sigma = H/L$, CDM coordinates locate the orbits of the reduced space as follows: the north pole of the sphere $\mathcal{S}(L, H)$, i.e., the point $E_0(0, 0, L^2(1-\sigma^2)/2)$, represents the circular orbits $(e = 0)$ with inclination $\cos I = \sigma$, whereas the south pole, i.e., the point of the sphere $E_3(0, 0, -L^2(1-\sigma^2)/2)$, represents the class of elliptic orbits with eccentricity $e = \sqrt{1-\sigma^2}$ in the equatorial plane. Finally any generic point $E(\xi_1, \xi_2, \xi_3)$ represents orbits with argument of periaxis

$$\cos g = \frac{\xi_1}{\sqrt{\xi_1^2 + \xi_2^2}}, \quad \sin g = \frac{\xi_2}{\sqrt{\xi_1^2 + \xi_2^2}}$$

and eccentricity $e = \sqrt{1 - G^2/L^2}$, where $G = \|\boldsymbol{G}\| = \sqrt{\xi_3 + L^2(1+\sigma^2)/2}$. In the limit $\sigma = 1$ the sphere is reduced to a point corresponding to equatorial circular orbit.

Applying Liouville's theorem $\dot{\xi}_i = \{\xi_i, \Lambda\}$, and rescaling the time, the global equations of motion are

$$(\dot{\xi_1}, \dot{\xi_2}, \dot{\xi_3}) = \frac{1}{G}(M_1\xi_2, -M_2\xi_1, M_3\xi_1\xi_2), \tag{4}$$

$$M_1 = 3\eta^2 + (1-\beta^2)\left(5c^2 - 4\eta^2 + \frac{5\xi_1^2}{G^2L^2}\right),$$

$$M_2 = 3\eta^2 + (1-\beta^2)\left(\eta^2 - \frac{5\xi_2^2}{G^2L^2}\right),$$

$$M_3 = \frac{10(1-\beta^2)}{L^2}.$$

where $\eta = G/L$, $c = H/G$. Notice that although σ is not explicit in (4), it is present through c^2 and η^2.

Our purpose is not to integrate the averaged equations, whose solutions can be expressed by elliptic functions, but rather to search for the relative equilibria as functions of the physical parameter β and the dynamical parameter σ.

The relative equilibria and their bifurcations are as follows.

(i) The poles E_0, E_3.—For any pair of values (β, σ) in the parameter plane, the right members of Eqs. (4) vanish for $\xi_1 = \xi_2 = 0$. So E_0, E_3 are always equilibria.

(ii) The points E_1, E_2 in the meridian circle $\xi_1 = 0$. —Setting (4) equal to zero, and assuming now $\xi_1 = 0$, we must have $M_1 = 0$, from which we get for ξ_3, or equivalently for η,

$$5\sigma^2(1-\beta^2) - (1-4\beta^2)\eta^4 = 0.$$

Then, keeping in mind the constraint $\sigma^2 \le \eta^2 \le 1$, and assuming $\beta \notin [\frac{1}{2}, 1]$, we get

$$\eta = [5\sigma^2(1-\beta^2)/(1-4\beta^2)]^{1/4}, \tag{5}$$

and finally from (3) we compute E_1, E_2. Moreover the limit value $\eta = 1$ lead(s) us to bifurcation lines N_1N_2, N_4N_6, given by $\sigma_1(\beta)$ corresponding to a pitchfork of the point E_0; from the other limit $\eta = \sigma$ we get the bifurcation line N_3N_4 given by $\sigma_2(\beta)$ which corresponds to a pitchfork of the point E_3:

$$\sigma_1(\beta) = \sqrt{\frac{1-4\beta^2}{5(1-\beta^2)}}, \qquad \sigma_2(\beta) = \sqrt{\frac{5(1-\beta^2)}{1-4\beta^2}}$$

(see Fig. 1) which also define different regions for the phase flow. In regions II and V we have two equilibria. In regions I, III, and IV we have four equilibria.

(iii) The points of the meridian circle $\xi_2 = 0$.—Again setting (4) equal to zero, and assuming now $\xi_2 = 0$, we must impose $M_2 = 0$ which leads to the relation for β:

$$\eta^2(4-\beta^2) = 0.$$

As we assume in this paper $m \ne 0$, which means that $\eta \ne 0$, we have roots only when $\beta = \pm 2$. Then, all the points in this meridian circle $\xi_2 = 0$ are equilibria.

This case is related to the line N_4N_5 in the parameter plane of global "oyster" bifurcations. We name the con-

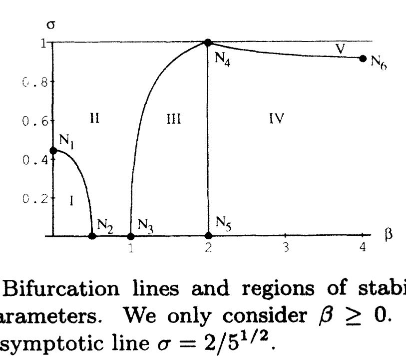

FIG. 1. Bifurcation lines and regions of stability in the plane of parameters. We only consider $\beta \ge 0$. By N_6 we mean the asymptotic line $\sigma = 2/5^{1/2}$.

figuration "oyster bifurcation," because in the neighborhood of $\beta = 2$ we see the two branches of the separatrix as valves hinging on E_0 or E_3 with the oyster closing its valves hinging on E_3 when we move in region III ($\beta < 2$) approaching the line N_4N_5, becoming the meridian circle $\xi_2 = 0$ when $\beta = 2$. In region IV ($\beta > 2$), the oyster opens its shells, but hinging now on the north pole E_0. As we will see from the stability analysis in the coming paragraphs, crossing the line N_4N_5 the north pole and the south pole switch their stability.

In summary, for the integrable cases $\beta = \frac{1}{2}, 1$, for any value of σ, there are two equilibria, E_0, E_3; for $\beta = 2$ we have a degenerate situation: all points on the meridian $\xi_2 = 0$ and $E_{1,2} = (0, \pm L^2\sqrt{\sigma}(1-\sigma), -L^2(1-\sigma)^2/2)$ in the meridian $\xi_1 = 0$ are equilibria. When $\sigma \sim 0$ we are near the south pole; when σ grows the equilibria move on the meridian towards the north but they remain always in the south hemisphere. For all the other values of β there are two equilibria E_0, E_3 and two more E_1,E_2 when $\sigma < \sigma_{1,2}(\beta)$.

Drawing the evolution of the energy at the different equilibria through the parameters gives us the stability of these points. Indeed, since for each pair (β, σ) the equilibria are over a compact, $\mathcal{S}^2$, the critical points which correspond to maximum and minimum values of the energy are stable, whereas critical points in which the energy takes an intermediate value, are unstable. The previous analysis suggests three distinguishable intervals according to the number of bifurcations: (a) $0 < \sigma < 1/\sqrt{5}$ (3 bifurcations), (b) $1/\sqrt{5} < \sigma < 2/\sqrt{5}$ (2 bifurcations), and (c) $2/\sqrt{5} < \sigma < 1$ (3 bifurcations). In Fig. 2, we represent the evolution of the energy at the equilibria for $\sigma = 0.2, 0.6, 0.95$, one for each of the previous intervals.

For $\sigma = 0.2$ we observe how the south pole E_3 (dashed line) is an absolute maximum value for the energy in the interval $0 \leq \beta < 1.012\,32$, an absolute minimum value of the energy in $2 < \beta$, and the energy in it takes an intermediate value in $1.012\,32 < \beta < 2$. Therefore, E_3 is unstable in this last interval, and stable in the complementary interval. In the same figure, the energy at the north pole E_0 (dotted line) takes an intermediate value with respect to the other critical points in $0 \leq \beta \leq 0.458\,83$, an absolute minimum in $0.458\,83 \leq \beta < 2$ and again, an intermediate value for $\beta > 2$. The critical points $E_{1,2}$ are absolute minima for the energy in $0 \leq \beta \leq 0.458\,83$, and absolute maxima in $\beta > 1.012\,32$, and they do not exist outside these intervals. Therefore, when they exist, they are stable points.

A similar analysis may be derived from other values of σ. Thus, in Fig. 2 for $\sigma = 0.6$, the energy at the north pole E_0 is minimum in $0 \leq \beta < 2$, and takes an intermediate value for $\beta > 2$. However, at the south pole E_3 is maximum in $0 \leq \beta < 1.141\,65$, intermediate in $1.141\,65 \leq \beta < 2$, and minimum in $\beta > 2$. The points $E_{1,2}$ only exist for $\beta \geq 1.141\,65$ and they are always maximum values of the energy.

Finally the lower part in Fig. 2 corresponds to $\sigma =$ 0.95. Since bifurcations occur in a narrow band, a close up of the picture is provided for observing the changes in stability. The north pole E_0 is an energy minimum in the interval $0 < \beta < 2$, E_0 takes an intermediate value in $2 \leq \beta < 2.617\,95$, and from this value on, the energy at E_0 is again maximum, and therefore, E_0 is stable for $\beta > 2.617\,95$. The south pole E_5 is unstable in $1.716\,39 \leq \beta < 2$ and stable in the rest. Finally the points $E_{1,2}$ exist for $1.716\,39 < \beta < 2.617\,95$ and the energy takes there the maximum value. Thus we have complemented in this way the analysis of Alhassid *et al.* (see Ref. [1], p. 1546) where they consider in detail the case $m = 0$.

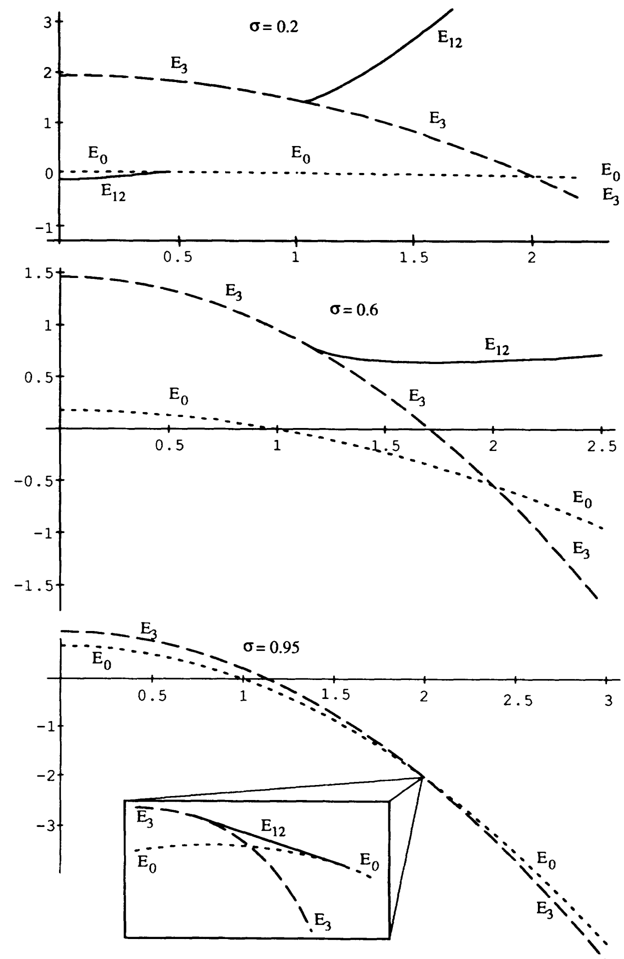

FIG. 2. Evolution of the energy at the equilibria as a function of β for $\sigma = 0.2$, 0.6, and 0.95.

We have determined (Fig. 3) the global picture of the dynamics of the Runge-Lenz vector: its libration and circulation modes. The trajectories are obtained not by integrating numerically the differential system, but simply by drawing the level contours of the manifold (2) on the sphere of radius $L^2(1-\sigma^2)/2$. The flow for each of the six domains (see Fig. 1) of the parameter plane is shown. In regions II and V the Runge-Lenz vector has

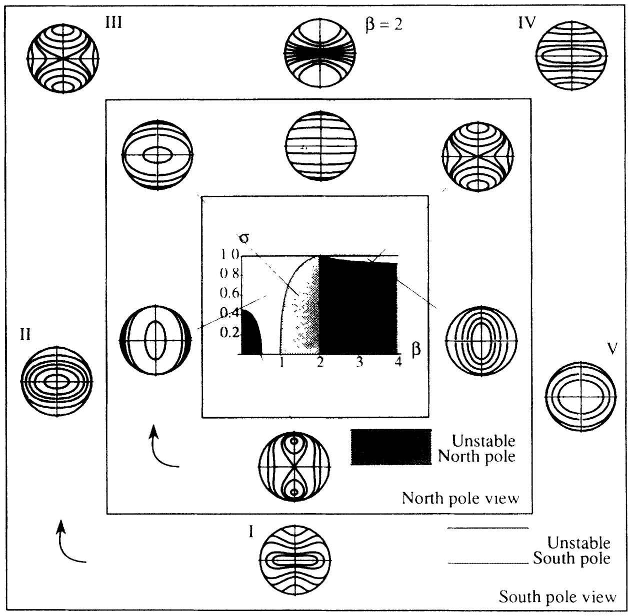

FIG. 3. Six different types of flow on S^2 over the parameter plane, showing north and south pole views. Notice that although the radius of the spheres are functions of σ we have presented all of them with the same radius.

only a circulation pattern. In regions I, III, and IV we see patterns of librations and rotations: circular (north pole) and equatorial (south pole) orbits have undergone pitchfork bifurcations crossing $\sigma < \sigma_1, \sigma_2$, respectively. The Zeeman effect ($\beta = 0$, region I) and the van der Waals case ($\beta = \sqrt{2}$, region III) belong to different regimes; in the Zeeman case Coffey *et al.* found the pitchfork for circular orbits at "critical inclination" $c = 1/\sqrt{5}$; we have shown here that in the van der Waals case there is a pitchfork bifurcation for equatorial orbits at a "critical eccentricity" $e = \sqrt{2/7}$, meanwhile circular orbits are stable. Finally, the phase portrait for $\beta = 2$ shows the Runge-Lenz vector having a pure libration pattern.

We now come to the question of integrability: Are there more integrals for this family of Hamiltonians (1)? Is there any way of getting new clues of integrability [20] from the averaged global flow? If the appearance-disappearance pattern of separatrices in the orbital space of the normalized system is taken as hinting at integrability [21], the study done here shows that the list consists only of the classical case $\beta = 1$ together with the other two recently found cases $\beta = \frac{1}{2}, 2$. Moreover, in the appearance-disappearance pattern of separatrices for the integrable cases we see also an explanation of the chaos-order-chaos behavior observed by Ganesan and Lakshmanan [10] in their quantum mechanical study of this problem.

We are extremely grateful to Dr. A. Deprit at the U. S. National Institute of Standards and Technology who introduced us to these techniques. This work was supported by Comisión Interministerial Científica y Técnica (CICYT PB90-0921 and ESP91-0919).

[1] Y. Alhassid, E. A. Hinds, and D. Meschede, Phys. Rev. Lett. **59**, 1545 (1987).

[2] J. C. Gay, in *Atoms in Unusual Situations*, edited by J. P. Briand, NATO ASI Ser. B, Vol. 143 (Plenum, New York, 1986), p. 1073.

[3] H. Hasegawa, M. Robnik, and G. Wunner, Prog. Theor. Phys. Suppl. **98**, 198 (1989).

[4] G. Baym, *Lectures on Quantum Mechanics* (Benjamin, New York, 1969), p. 234.

[5] K. Ganesan and M. Lakshmanan, Phys. Rev. Lett. **62**, 232 (1989); Phys. Rev. A **42**, 394 (1990).

[6] J. Milligan and D. Farrelly, Phys. Rev. A **47**, 3137 (1993).

[7] A. Elipe and S. Ferrer, *Hamiltonian Dynamical Systems: History, Theory, and Application*, IMA Series (Springer, Berlin, to be published).

[8] J. E. Howard and D. Farrelly, Phys. Lett. A **178**, 62 (1993); D. Farrelly and J. E. Howard, Phys. Rev. A **48**, 851 (1993).

[9] R. Blümel, C. Kappler, W. Quint, and H. Walther, Phys. Rev. A **40**, 808 (1989); **46**, 8034(E) (1992).

[10] K. Ganesan and M. Lakshmanan, Phys. Rev. A **45**, 1548 (1992); **48**, 964 (1993).

[11] H. Goldstein, *Classical Mechanics* (Addison-Wesley, Reading, MA, 1980), p. 483.

[12] T. Uzer, D. Farrelly, J. Milligan, P. Raines, and J. Skelton, Science **253**, 42 (1991).

[13] E. A. Solov'ev, Pis'ma Zh. Eksp. Teor. Fiz. **34**, 278 (1981) [JETP Lett. **34**, 265 (1981)].

[14] D. R. Herrick, Phys. Rev. A **26**, 323 (1982).

[15] K. Moser, Commun. Pure Appl. Math. **23**, 609 (1970); V. Fock, Z. Phys. **98**, 145 (1936)

[16] K. R. Meyer, in *Dynamical Systems*, edited by M. M. Peixoto (Academic Press, New York, 1973), p. 259.

[17] J. E. Marsden, *Lectures on Mechanics*, London Mathematical Society Lecture Note Series 174 (Cambridge Univ. Press, Cambridge, 1992); J. E. Marsden and A. Weinstein, Rep. Math. Phys. **5**, 121 (1974).

[18] W. G. Harter and C. W. Patterson, J. Chem. Phys. **80**, 4241 (1984); M. E. Kellman and E. D. Lynch, J. Chem. Phys. **88**, 2205 (1988)

[19] S. Coffey *et al.*, Ann. N.Y. Acad. Sci. **497**, 22 (1987); S. Coffey, A. Deprit, and B. R. Miller, Celest. Mech. **39**, 365 (1987); S. Coffey *et al.*, Science **247**, 833 (1990).

[20] D. Farrelly and T. Uzer (to be published) have gone up to tenth order looking for the relation between separability and degeneracy of the normalized Hamiltonian.

[21] We find more evidence of this in perturbed elliptic oscillators: S. Ferrer *et al.*, Phys. Lett. A **146**, 411 (1990); A. Deprit and A. Elipe, Celest. Mech. **51**, 227 (1991).

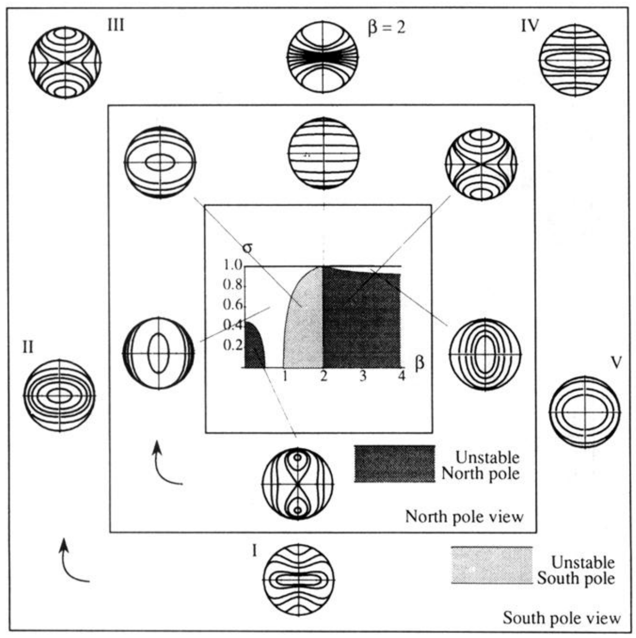

FIG. 3. Six different types of flow on S^2 over the parameter plane, showing north and south pole views. Notice that although the radius of the spheres are functions of σ we have presented all of them with the same radius.